SOILS AND FOUNDATIONS Vol. 24, No. 3, 27-40, Sept. 1984
Japanese Society of Soil Mechanics and Foundation Engineering

ELASTIC COMPLIANCE FOR ROCK-LIKE MATERIALS WITH RANDOM CRACKS

MASANOBU ODA* KENICHIRO SUZUKI** and TAKURO MAESHIBU**

ABSTRACT

Elastic compliances for cracked materials like rocks and rock masses are theoretically formulated in terms of the generalized fabric tensor which has been introduced as an index measure to express explicity crack geometry. By means of uniaxial compression tests and supersonic wave velocity tests on gypsum plaster samples with random cracks, the formulation is proved to give a good approximation for describing the elastic response of cracked materials. The conclusions are summarized as follows: The principal axes of the fabric tensor of second-rank exactly coincide with the symmetry axes of the elastic compliance tensor of fourth-rank. The so-called self-consistent method is very useful to estimate the overall elastic moduli by taking into account the effect of elastic interaction among cracks. Since the supersonic wave velocity is closely related to the character of the fabric tensor, it can be expected that the field measurement of wave velocity is useful to estimate fabric tensor of in situ rock masses.

Key words : anisotropy, elasticity, faults, joint, model test, rock mass, stress-strain curve, unconfined compression test (**IGC** : F 3/F 6)

INTRODUCTION

Faults and joints (called cracks) are of widespread occurrence in rocks and rock masses. For the past two decades, extensive studies have been done to estimate with sufficient accuracy the effect of cracks on the stability of engineering structures constructed on or in rock masses: Several computer models, for example, have been successfully developed to replace cracks by mechanically equivalent elements; e. g., Goodman, et al. (1968), Zienkiewicz and Dullage (1970), Cundall (1971) and Kawai and Takeuchi (1983). In laboratories, on one hand, a great effort has been paid to make it clear the important influence of crack system (crack geometry) on mechanical properties of cracked materials; e. g., Hayashi (1966), Brown (1970) and Einstain and Hirschfeld (1973). In spite of these remarkable studies, however, a great difficulty still exists in developing idealized models mechanically equivalent to real rock masses which are commonly characterized by very complicated geological setting of cracks, especially in crack geometry; e. g., John (1962), Hansagi (1974), Silveria, Rodrigues

* Associate Professor, Department of Foundation Engineering, Saitama University, Urawa, Saitama.
** Graduate Students, ibid.

Manuscript was received for review on October 17, 1983.
Written discussions on this paper should be submitted before April 1, 1985, to the Japanese Society of Soil Mechanics and Foundation Engineering, Sugayama Bldg. 4 F, Kanda Awaji-cho 2-23, Chiyoda-ku, Tokyo 101, Japan. Upon request the closing date may be extended one month.

and Grossmann (1966), Kiraly (1965), Ogata (1978) and Hudson and Priest (1983).

In order to overcome the present difficulty, Oda (1984) proposed a tensor quantity called the generalized fabric tensor to represent crack geometry (crack system) in general form. This paper is to discuss the following two topics: (1) A new stress-strain relation which is easily incorporated into conventional FEM analyses is formulated in terms of the generalized fabric tensor by treating cracked bodies as elastically anisotropic solids, and (2) results of uniaxial compression tests and supersonic velocity tests on gypsum plaster samples with various kinds of cracks are reported to see if the elastic constitutive equation is accurate enough to be used in deformation analyses of rock masses.

CRACKS

Modeling of Cracks

Cracks appear in various scales ranging from micro-cracks visible through a scanning electron microscope to great faults extending for several hundred kilometers. Because of the variety of natural cracks, it is almost impossible to replace them by an equivalent model without losing generality. If elastic behavior is only concerned, however, a crack can be modeled either by a penny-shaped opening or by a row of collinear openings (Fig. 1(a) and (b)). The models are justified by the following observations:

1) Fig. 2 is typical of cracks visible on thin sections sliced from two moderately weathered granites. The crack in Fig. 2

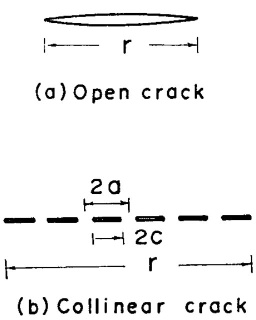

Fig. 1. Idealized models of cracks

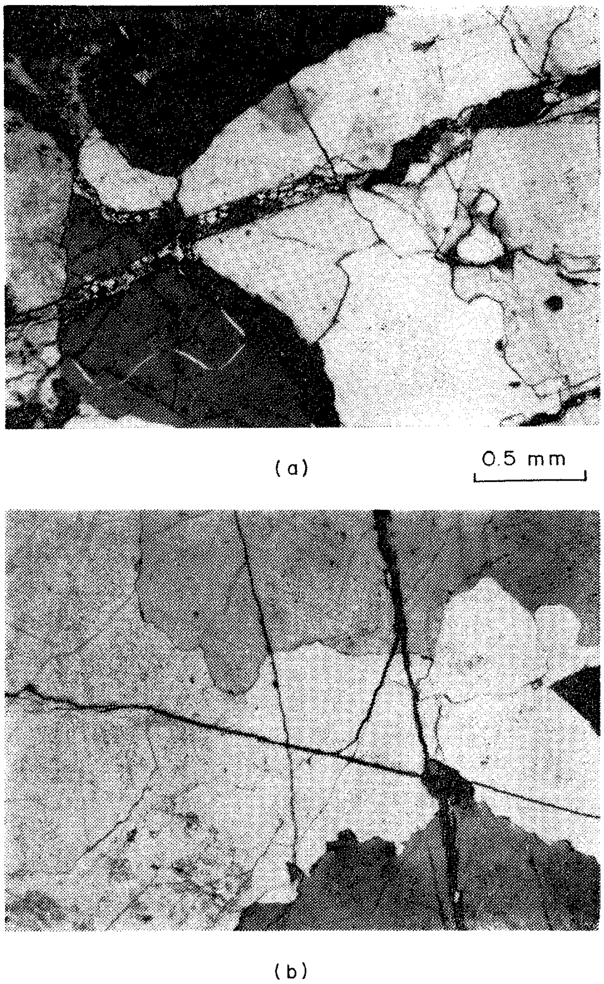

Fig. 2. Cracks in weathered granites (A large crack extending from the left to the right of picture (a) is part of a joint commonly observed in a moderately weathered granite having porosity of 11.4%. It is clearly seen that the crack is filled with clay minerals such as vermiculite and illite. Picture (b) is taken from a slightly weathered granite having porosity of 2.8%. There are many micro-cracks filled with fine particles stained by brownish color)

(a) is part of a joint stained by brownish color. Note that these cracks are filled with clay minerals such as vermiculite and illite which were derived from weathering products or fault gouge (Onodera, Yoshinaka and Oda, 1974). The filling materials are characterized not only by high compressibility, but also by low shear strength, especially when they are saturated with water. Let us image what happens if these cracks are stressed. It is not probable that they behave as completely closed cracks developing high friction on their surfaces. Their elastic response can be rather well reproduced by the models of Fig. 1.

2) Sprunt and Brace (1974) directly observed micro-cavities in crystalline rocks by a scanning electron microscope. According to their observation, a single crack with high aspect ratio is actually a string of many low aspect ratio cavities, with the appearance similar to the model of Fig. 1(b).

Crack Geometry

In order to define explicitly crack geometry, we must consider at least the following three factors:

1) Volume density of cracks: When there are $m^{(V)}$ cracks in volume V, volume density ρ of cracks is defined as the number of cracks in a unit volume; i. e., $\rho=m^{(V)}/V$.

2) Dimension of cracks: If each flat crack is identified by its typical dimension r, the distribution of the crack sizes is then characterized by a density function $f(r)$.

3) Orientation of cracks: Orientation of a crack is specified by two unit vectors, $\boldsymbol{n}^{(+)}$ and $\boldsymbol{n}^{(-)}$, normal to its major principal plane (Fig. 3). Since $E(\boldsymbol{n}, r)$ is introduced as a density function for representing the distribution of $\boldsymbol{n}$, it satisfies

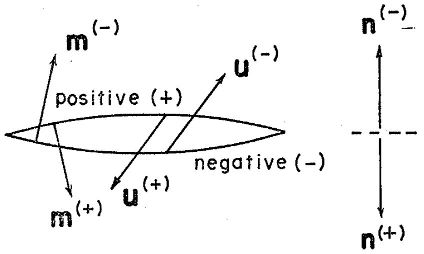

Fig. 3. Displacement vectors $\boldsymbol{u}^{(+)}$ and $\boldsymbol{u}^{(-)}$ associated with positive (+) and negative (−) surfaces respectively (Note the difference between $\boldsymbol{m}$ and $\boldsymbol{n}$. That is, $\boldsymbol{m}$ is a unit vector normal to a crack surface while $\boldsymbol{n}$ is a unit vector normal to the major plane of the crack)

$$\int_0^\infty \int_\Omega E(\boldsymbol{n}, r)\,d\Omega dr = \int_0^\infty \int_{\Omega/2} 2E(\boldsymbol{n}, r)\,d\Omega dr = 1 \qquad (1)$$

where Ω and $\Omega/2$ are solid angles showing the limits of integration; Ω=an entire unit sphere, and $\Omega/2$=a unit hemisphere. $E(\boldsymbol{n}, r)$ is symmetric in the sense of $E(\boldsymbol{n}, r)=E(-\boldsymbol{n}, r)$, and is written as $E(\boldsymbol{n})f(r)$ if $\boldsymbol{n}$ and r are statistically independent.

By taking into account the three elements described above, a tensor $\boldsymbol{F}$ (called the generalized fabric tensor) is defined as

$$\boldsymbol{F}=\frac{\pi\rho}{4}\int_0^\infty \int_\Omega r^3 \boldsymbol{n}\otimes\boldsymbol{n}\cdots\otimes\boldsymbol{n}E(\boldsymbol{n}, r)\,d\Omega dr \qquad (2)$$

where $\otimes$ stands for tensor product (Oda, 1984). The generalized fabric tensor is a dimensionless tensor with even rank. (Because of the symmetry, $E(\boldsymbol{n}, r)=E(-\boldsymbol{n}, r)$, $\boldsymbol{F}$ is identically zero if the rank is odd.) Its components are symmetric in the sense of $F_{ij\cdots k}=F_{ji\cdots k}=\cdots=F_{kj\cdots i}$. A contraction with respect to any pair of subscripts reduces its rank by 2. The zero-, second- and fourth- rank tensors, for example, are given below where a fixed rectangular Cartesian coordinate system is used:

Zero-rank:
$$F_0=\frac{\pi\rho}{4}\int_0^\infty r^3 f(r)\,dr \qquad (3a)$$

Second-rank:
$$F_{ij}=\frac{\pi\rho}{4}\int_0^\infty \int_\Omega r^3 n_i n_j E(\boldsymbol{n}, r)\,d\Omega dr \qquad (3b)$$

Fourth-rank:
$$F_{ijkl}=\frac{\pi\rho}{4}\int_0^\infty \int_\Omega r^3 n_i n_j n_k n_l E(\boldsymbol{n}, r)\,d\Omega dr \quad (i, j, k, l=1, 2, 3) \qquad (3c)$$

The zero-rank tensor F_0 is a scalar quantity equivalent to the crack concentration parameter by Budiansky and *O'Connell* (1976), and is also related to porosity associated with cracks (Oda, 1984). The second-rank tensor corresponds not only to the crack density tensor α_{ij} by Kachanov (1980), but also to the fabric tensor by Oda (1982). Fabric tensors of higher ranks than F_{ij} are not directly related to an image of the crack geometry. It can be intuitively said, however, that the detail of the crack geometry can be better represented if higher rank tensors are considered. Let us consider, for example, two cracked bodies having a common fabric tensor of $2n$-th rank. These bodies cannot be distinguished by means of fabric tensors of rank lower than $2n$-th. If the higher rank tensors than $2n$-th are taken into account, however, two bodies may no longer appear identical.

It must be emphasized here that the generalized fabric tensor for rock masses was explicity written in terms of some quantities measurable in conventional geological surveys by Oda (1983, 1984). Accordingly, attention is paid here only to formulate an equation of elastic compliance for cracked bodies by using the generalized fabric tensor.

ELASTIC COMPLIANCE FOR CRACKED BODIES

Many theoreticians have been interested in formulating overall modulus of rock-like materials by considering the effect of cracks on their elasticity; e.g., Walsh (1965 a, b) Jaeger and Cook (1969), Budiansky and O'Connell (1976), Eimer (1978), Kachanov (1980, 1982), Oda (1983) Horii and Nemat-Nasser (1983) and Horii (1983). They considered isotropically distributed ellipsoids or penny-shaped cracks in an elastically isotropic solid. Recent progress has been achieved by employing the so-called self-consistent method by which elastic interaction between cracks can be taken into account; e.g., Budiansky and O'Connell (1976) and Horii and Nemat-Nasser (1983).

General Formulation

Let us consider an elastic solid of total volume V containing $m^{(V)}$ cracks. Average stress tensor $\bar{\sigma}_{ij}$ of

$$\bar{\sigma}_{ij}=\frac{1}{V}\int_V \sigma_{ij}dV \tag{4}$$

produces average strain tensor $\bar{\varepsilon}_{ij}$ of

$$\bar{\varepsilon}_{ij}=\frac{1}{V}\int_V \varepsilon_{ij}dV$$

$$=\frac{1}{V}\int_V \frac{1}{2}(u_{i,j}+u_{j,i})dV \qquad (i, j=1,2,3) \tag{5}$$

where u_i $(i=1,2,3)$ are components of a displacement vector, and comma followed by an index denotes partial differential with respect to the corresponding coordinate. The average strain tensor is related to the average stress tensor through an elastic compliance tensor $\bar{D}_{ijkl}$ as follows;

$$\bar{\varepsilon}_{ij}=\bar{D}_{ijkl}\bar{\sigma}_{kl} \quad (i, j, k, l=1,2,3) \tag{6}$$

$\bar{D}_{ijkl}$ consists of two parts: The first $\bar{M}_{ijkl}$ depends on the elasticity of matrix without any crack, while the second $\bar{C}_{ijkl}$ is the correction due to the existence of cracks; i.e.,

$$\bar{D}_{ijkl}=\bar{M}_{ijkl}+\bar{C}_{ijkl} \tag{7}$$

If an elastically isotropic matrix is only concerned, then $\bar{M}_{ijkl}$ is given by

$$\bar{M}_{ijkl}=\frac{(1+\nu)}{E}\delta_{ik}\delta_{jl}-\frac{\nu}{E}\delta_{ij}\delta_{kl} \tag{8}$$

where E and ν are Young's modulus and Poisson's ratio respectively, and δ_{ij} is Kronecker's delta. Horii and Nemat-Nasser (1983) theoretically showed that $\bar{C}_{ijkl}$ satisfies

$$\bar{C}_{ijkl}\bar{\sigma}_{kl}=\frac{1}{V}\int_{2S}\frac{1}{2}(u_i m_j+u_j m_i)ds \tag{9}$$

where m_i $(i=1,2,3)$ are components of a unit vector normal to crack surfaces, and $2S$ is the total surface area of $m^{(V)}$ cracks. (A k-th crack among $m^{(V)}$ cracks consists of two surfaces, positive(+) and negative (−), each of which has an area $S^{(k)}$. Then the total area $2S$ of all cracks is the summation of $\sum_{(k)=1}^{m^{(V)}} 2S^{(k)}$.)

Instead of integrating the right side of Eq. (9) for all cracks, a k-th crack is first chosen to see its effect on $\bar{C}_{ijkl}$, and afterwards each effect is summed: Since the k-th crack is assumed to be flat in its shape, the unit normal vector $\boldsymbol{m}$ is oriented almost parallel to a unit vector $\boldsymbol{n}$ defining a general normal trend of the crack. Integration of Eq. (9) only for the k-th crack becomes

$$\frac{1}{2V}\int_{2S^{(k)}}(u_j m_i+u_i m_j)ds$$
$$=\frac{1}{2V}\left[n_i\int_{2S^{(k)}}u_j ds+n_j\int_{2S^{(k)}}u_i ds\right]$$
$$=\frac{S^{(k)}}{2V}(n_i\bar{\delta}_j+n_j\bar{\delta}_i) \qquad (10)$$

where $\bar{\delta}_i$ is to denote the mean displacement jump defined by

$$\bar{\delta}_i=\frac{1}{S^{(k)}}\int_{S^{(k)}}(u_i^{(+)}-u_i^{(-)})ds$$
$$=\frac{1}{S^{(k)}}\int_{2S^{(k)}}u_i ds \qquad (11)$$

Here $u_i^{(+)}$ and $u_i^{(-)}$ $(=-u_i^{(+)})$ are for the displacements on the positive(+) and the negative(−) surfaces respectively (Fig. 3).

Next, consider a number dN of cracks (in volume V) having unit normal vectors oriented inside a small solid angle $d\Omega$ around $\boldsymbol{n}$, and also having sizes within a small range from r to $r+dr$ (called $(\boldsymbol{n}, r)$-cracks). The number results from multiplying the total number $m^{(V)}$ of cracks by the rate of the $(\boldsymbol{n}, r)$-cracks:

$$dN=2\,m^{(V)}E(\boldsymbol{n}, r)d\Omega dr \qquad (12)$$

On the assumption that elastic interaction between cracks is negligibly small, the effect of each $(\boldsymbol{n}, r)$-crack on $\bar{C}_{ijkl}$ is simply summed to find the total effect of all $(\boldsymbol{n}, r)$-cracks, as follows:

$$\frac{\rho}{2}S(r)(n_i\bar{\delta}_j+n_j\bar{\delta}_i)2\,E(\boldsymbol{n}, r)d\Omega dr \qquad (13)$$

Integrating Eq. (13) over $0\leqq\Omega/2\leqq2\pi$ and $0\leqq r<\infty$, it becomes the right side of Eq. (9) since all cracks $m^{(V)}$ are taken into account. Then we have

$$\bar{C}_{ijkl}\bar{\sigma}_{kl}=\frac{\rho}{2}\int_0^\infty\int_{\Omega/2}S(r)(n_i\bar{\delta}_j+n_j\bar{\delta}_i)2\,E(\boldsymbol{n}, r)d\Omega dr \qquad (14)$$

Accordingly, it can be said that the compliance $\bar{C}_{ijkl}$ is formulated in terms of the mean displacement jumps $\bar{\delta}_i$ associated with all cracks.

Displacement Jump

Local base vectors $\boldsymbol{e}_i'$ $(i=1, 2, 3)$ are set with respect to a crack as follows: $\boldsymbol{e}_1'$ is normal to the major plane of the crack ($\boldsymbol{e}_1'/\!/\boldsymbol{n}$) and $\boldsymbol{e}_2'$ and $\boldsymbol{e}_3'$ are in the plane. The unit vectors $\boldsymbol{e}_1'$, $\boldsymbol{e}_2'$ and $\boldsymbol{e}_3'$ make a right hand system in the order, and are related to fixed base vectors $\boldsymbol{e}_i$ $(i=1, 2, 3)$ by

$$\boldsymbol{e}_i'=Q_{ij}\boldsymbol{e}_j \qquad (15)$$

where Q_{ij} is an orthogonal (rotational) tensor.

Here, four examples are discussed to seek a general character related to the displacement jump:

1) *Penny-shaped crack*: In this case, the displacement jump is written as

$$\bar{\delta}_1'=\frac{8(1-\nu^2)}{3\pi E}r\bar{\sigma}_{11}' \qquad (16\text{ a})$$
$$\bar{\delta}_2'=\frac{16(1-\nu^2)}{3\pi E(2-\nu)}r\bar{\sigma}_{12}' \qquad (16\text{ b})$$
$$\bar{\delta}_3'=\frac{16(1-\nu^2)}{3\pi E(2-\nu)}r\bar{\sigma}_{13}' \qquad (16\text{ c})$$

where $\bar{\delta}_i'$ and $\bar{\sigma}_{ij}'$ are components with respect to the local base vectors $\boldsymbol{e}_i'$ $(i=1, 2, 3)$ (Oda, 1983). For a rather special case having $\nu=0$, Eq. (16) can be rewritten with respect to the fixed base vectors $\boldsymbol{e}_i$ $(i=1, 2, 3)$ as

$$\bar{\delta}_i=\frac{8}{3\pi E}r\bar{\sigma}_{ij}n_j \qquad (17)$$

Since Eq. (17) greatly simplifies the integration of Eq. (14) without any serious error, it is accepted here as a possible expression for the displacement jump of penny-shaped crack.

2) *Elliptical crack*: In the case of an elliptical crack subjected to the plane stress, the jump is exactly given by

$$\bar{\delta}_i=\frac{\pi}{2E}r\bar{\sigma}_{ij}n_j \qquad (18)$$

without making any simplification (e. g., Walsh, 1965; Oda, 1983).

3) *Row of collinear cracks*: In this case, a crack having apparent crack length r is actually a row of many collinear cracks (Fig. 1(b)). Let us assume that the elastic solution for an infinite row of collinear cracks subjected to the plane stress (e. g., Sneddon and Lowengrub, 1969) can be used to roughly estimate the displacement jump associated with a finite row of collinear

cracks. It seems reasonable to assume further that a, a length allocated to a collinear crack in Fig. 1(b), is proportional to r; i.e., $a=kr$. This is probable because a crack having larger apparent crack length consists of larger collinear cracks. If the two assumptions are accepted, the displacement jump becomes

$$\bar{\delta}_i=\frac{1}{K}r\bar{\sigma}_{ij}n_j \tag{19}$$

where

$$\frac{1}{K}=\frac{8k}{\pi E}\log\left(\sec\frac{\pi c}{2a}\right).$$

4) *Experiment*: Yoshinaka, Yamabe and Sekine (1982) have studies experimentally the displacement jump associated with an artificial crack. Increments of normal stress $\Delta\bar{\sigma}_n$ and shear stress $\Delta\bar{\tau}$ are applied on a crack with successive measurements of associated displacement jumps $\Delta\bar{\delta}_n$ and $\Delta\bar{\delta}_s$ corresponding to the normal and the shear stress directions respectively. Then they calculated the normal G_n and the shear G_s stiffnesses defined by

$$G_n=\frac{\Delta\bar{\sigma}_n}{\Delta\bar{\delta}_n},\quad G_s=\frac{\Delta\bar{\tau}}{\Delta\bar{\delta}_s} \tag{20}$$

Their experimental results suggest that G_n equals G_s if the increments are limited to the elastic range without large permanent slip along a crack; i.e., $\Delta\bar{\sigma}_n/\Delta\bar{\tau}=\Delta\bar{\delta}_n/\Delta\bar{\delta}_s$. This means that the jump vector $\bar{\boldsymbol{\delta}}$ is parallel to a traction vector $\bar{\boldsymbol{T}}$ acting on a crack. They also reported that the shear stiffness G_s is reciprocally proportional to crack area. Accordingly, the associated jump is proportional to crack length. Taking into account these two evidences, we have

$$\Delta\bar{\delta}_i=\frac{1}{D}r\Delta\bar{\sigma}_{ij}n_j \tag{21}$$

where $1/D$ is no longer constant, but depends nonlinearly on normal stress acting on a crack. (This is due to closure of the crack which causes the increase of stiffness. Of course, it is very important to consider the closure especially when stress-dependent elasticity of rock-like materials is concerned. For simplicity, however, this problem is not discussed here anymore.) It is interesting to notice, however, that Eq. (21) is quite similar to Eqs. (17) to (19) in the structure of equations.

In conclusion, the displacement jump can be formulated in the form of

$$\bar{\delta}_i=\frac{1}{D}r\bar{\sigma}_{ij}n_j \tag{22}$$

Using this in Eq. (14), we have

$$\begin{aligned}\bar{C}_{ijkl}&=\frac{\pi\rho}{8D}\int_0^\infty\int_{\Omega_2}r^3(n_in_k\delta_{jl}+n_jn_l\delta_{ik})\\&\quad\times 2E(\boldsymbol{n},r)d\Omega dr\\&=\frac{1}{4D}(\delta_{il}F_{jk}+\delta_{jl}F_{ik}+\delta_{jk}F_{il}+\delta_{ik}F_{jl})\end{aligned} \tag{23}$$

Where $S(r)$ is set as $(\pi/4)r^2$ in the case of penny-shaped crack, and F_{ij} is the fabric tensor of second-rank (Eq. (3b)).

From Eqs. (6), (7), (8) and (23), an elastic stress-strain relation is finally given in matrix form as

$$\begin{bmatrix}\bar{\varepsilon}_{11}\\\bar{\varepsilon}_{22}\\\bar{\varepsilon}_{33}\\\bar{\varepsilon}_{23}\\\bar{\varepsilon}_{31}\\\bar{\varepsilon}_{12}\end{bmatrix}=\frac{1}{D}\begin{bmatrix}F_{11}+\frac{D}{E} & -\frac{D}{E}\nu & -\frac{D}{E}\nu & 0 & \frac{1}{2}F_{13} & \frac{1}{2}F_{12}\\ & F_{22}+\frac{D}{E} & -\frac{D}{E}\nu & \frac{1}{2}F_{23} & 0 & \frac{1}{2}F_{12}\\ & & F_{33}+\frac{D}{E} & \frac{1}{2}F_{23} & \frac{1}{2}F_{31} & 0\\ & & & \frac{F_{22}+F_{33}}{4}+\frac{D}{4G} & \frac{1}{4}F_{12} & \frac{1}{4}F_{31}\\ & & & & \frac{F_{33}+F_{11}}{4}+\frac{D}{4G} & \frac{1}{4}F_{23}\\ & \text{(Symmetrical)} & & & & \frac{F_{11}+F_{22}}{4}+\frac{D}{4G}\end{bmatrix}\begin{bmatrix}\bar{\sigma}_{11}\\\bar{\sigma}_{22}\\\bar{\sigma}_{33}\\2\bar{\sigma}_{23}\\2\bar{\sigma}_{31}\\2\bar{\sigma}_{12}\end{bmatrix} \tag{24}$$

Eq. (24) gives an elastic compliance $\bar{D}_{ijkl}$ in terms of the fabric tensor, with the following two important characters: (1) The symmetry axes of the fourth-rank tensor $\bar{D}_{ijkl}$ exactly coincide with the principal axes of the fabric tensor F_{ij}. (Let the reference axes be the principal axes of F_{ij}; i.e., $F_{12}=F_{23}=F_{31}=0$. It is easily seen that the elastic compliance of Eq. (24) is reduced to that for a body with rhombic symmetry three symmetry axes of which accord with the reference axes.) (2) $\bar{D}_{ijkl}$ is symmetric in the sense of

$$\bar{D}_{ijkl}=\bar{D}_{jikl}=\bar{D}_{ijlk}=\bar{D}_{klij} \quad (25)$$

It is worthy of note again that Eq. (24) is based on the assumption that the elastic interaction between cracks is negligibly small. This assumption becomes serious especially when the crack density is high. The restriction will be overcome, as will be seen later, if the self-consistent method is adopted.

EXPERIMENTAL STUDY

For the purpose of checking the applicability of Eq. (24) to rock-like materials, unconfined compression tests and supersonic velocity tests are performed on gypsum plaster samples including two-dimensional cracks.

Experimental Procedures

Experimental procedures are as follows: (1) Position and orientation of two-dimensional cracks are previously determined. (2) Water-gypsum mixture (2 : 3 by weight) is poured into a rectangular prismatic mold or into a cylindrical mold with a circular cross section. (3) Strips made of greased picture postcards are inserted into the water-gypsum mixture at previously selected positions with previously selected orientations. Since the greased picture postcards are so soft as compared with hardened plaster gypsum, they are expected to act as open cracks under stresses. In one experimental series, the inserted postcards are pulled out afterwards

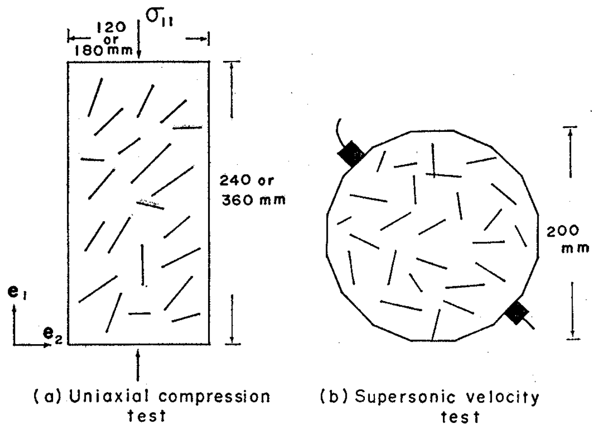

Fig. 4. Samples for a uniaxial compression test and for a supersonic wave velocity test

to make real open cracks. It is proved that there is no distinction between the greased postcard and the real open crack in their mechanical response. (4) After about an hour, the well-hardened water-gypsum mixture is taken out of the molds, and is trimmed to make a rectangular prism or an equilateral polygon (Fig. 4). The former is for a unconfined compression test and the later for a supersonic velocity test. (5) The samples thus made are cured for about three weeks in a constant temperature and humidity room.

Result of Unconfined Compression Tests

Base vectors $\boldsymbol{e}_i$ ($i=1, 2$) are fixed to a longitudinal and a transversal directions of each sample respectively (Fig. 4(a)). Since uniaxial stress is increased vertically downward, it is labeled as $\bar{\sigma}_{11}$. To determine complete strain tensor (two-dimensional), three extensional strains are at least measured by the following procedures: Several markers are glued on a surface of a sample, and the change of the distances between them is measured step by step by a contact gauge with accuracy of 1/1 000 millimeter.

Relations between axial stress $\bar{\sigma}_{11}$, axial strain $\bar{\varepsilon}_{11}$ and lateral strain $\bar{\varepsilon}_{22}$ are shown in Fig. 5 for two samples (A) and (B) whose fabric tensors are

$$F_{ij}^{(A)}=\begin{bmatrix} F_{11} & F_{12} \\ F_{21} & F_{22} \end{bmatrix}=\begin{bmatrix} 0 & 0 \\ 0 & 0.309 \end{bmatrix}$$

and

$$F_{ij}^{(B)}=\begin{bmatrix}0.189 & 0.028\\ 0.028 & 0.253\end{bmatrix}$$

respectively. Note that both samples deform elastically until the axial stress $\bar{\sigma}_{11}$ reaches the fifty percent of the ultimate value. When new cracking begins to initiate from pre-existing cracks, as shown by arrows in Fig. 5, the lateral extension $\bar{\varepsilon}_{22}$ suddenly increases.

Our interest is limited to the elastic range of materials in the following discussion. Elastic constants, if necessary, are calculated by applying the least square method to the linear portion of stress-strain curves.

If the greased postcards behave as open-elliptical cracks, $1/D$ equals $\pi/(2E)$ and the two-dimensional version of Eq. (24) becomes

$$\begin{bmatrix}\bar{\varepsilon}_{11}\\ \bar{\varepsilon}_{22}\\ \bar{\varepsilon}_{12}\end{bmatrix}=\frac{1}{E}\begin{bmatrix}\frac{\pi}{2}F_{11}+1 & -\nu & \frac{\pi}{4}F_{12}\\ & \frac{\pi}{2}F_{22}+1 & \frac{\pi}{4}F_{12}\\ \text{(Symmetrical)} & & \frac{\pi}{8}(F_{11}+F_{22})+\frac{(1+\nu)}{2}\end{bmatrix}\begin{bmatrix}\bar{\sigma}_{11}\\ \bar{\sigma}_{22}\\ 2\bar{\sigma}_{12}\end{bmatrix} \qquad (26)$$

Taking into account $\bar{\sigma}_{11}\neq 0$ and $\bar{\sigma}_{22}=\bar{\sigma}_{12}=0$ for a uniaxial compression test, Eq. (26) is further simplified as

$$\frac{\bar{\sigma}_{11}}{\bar{\varepsilon}_{11}}=E'=\frac{E}{\frac{\pi}{2}F_{11}+1} \qquad (27a)$$

$$-\frac{\bar{\varepsilon}_{22}}{\bar{\varepsilon}_{11}}=\nu'=\frac{\nu}{\frac{\pi}{2}F_{11}+1} \qquad (27b)$$

Note that E' and ν' defined by Eq. (27) are apparent elastic coefficients for an elastically anisotropic material.

If a sample is isotropic in the sense of $F_{ij}=1/2F_0\delta_{ij}$, Eq. (27) can be rewritten in terms of the fabric tensor F_0 of zero-rank as

$$\bar{E}=\frac{E}{\frac{\pi}{4}F_0+1} \qquad (28a)$$

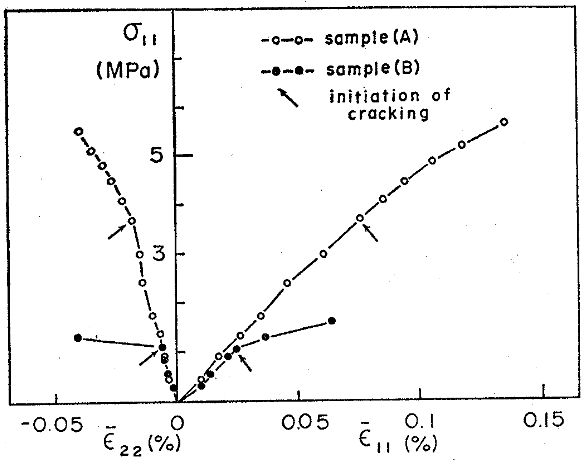

Fig. 5. The relations between axial stress $\bar{\sigma}_{11}$, axial strain $\bar{\varepsilon}_{11}$ and lateral strain $\bar{\varepsilon}_{22}$ for two samples (A) and (B) (Note that the stress-strain curves are linearly elastic until new cracking begins to initiate from pre-existing cracks, as clearly shown by arrows in the figure)

$$\bar{\nu}=\frac{\nu}{\frac{\pi}{4}F_0+1} \qquad (28b)$$

where $\bar{E}$ and $\bar{\nu}$ are a complete set of the elastic constants for the isotropic, cracked material.

Experimental results of the elastic coefficients E' and ν' are shown in Figs. 6

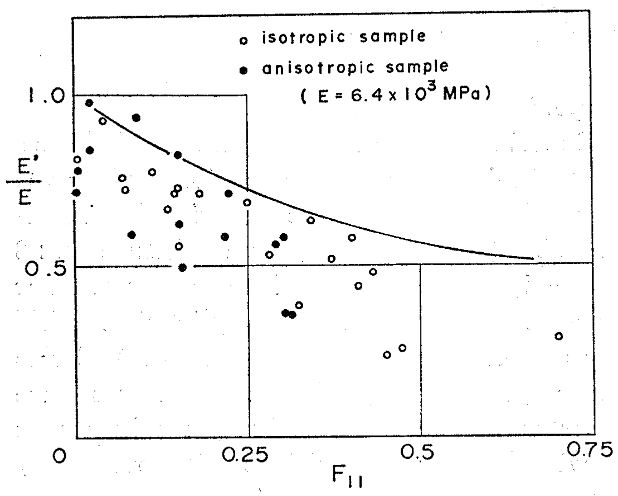

Fig. 6. The effect of the fabric tensor on the apparent Young's modulus E' of cracked bodies (Note that Eq. (27a) is not exact to follow the experimental results, but rather gives an upper bound)

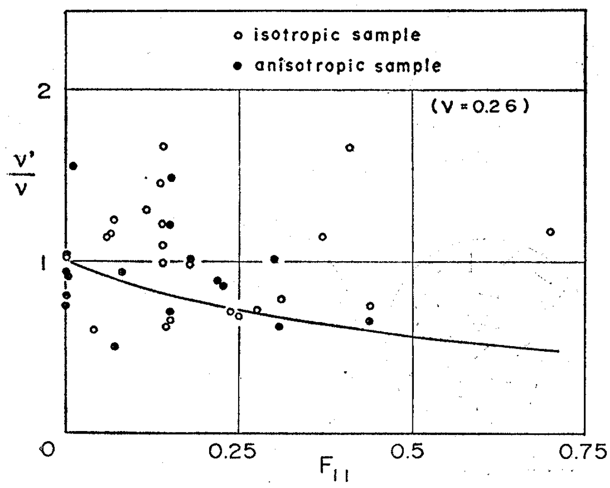

Fig. 7. The effect of the fabric tensor on the apparent Poisson's ratio ν' of cracked bodies

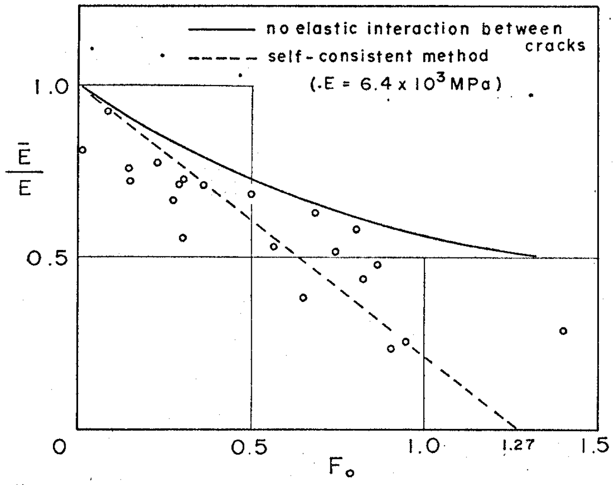

Fig. 8. The effect of the zero-rank fabric tens F_0 on Young's modulus $\bar{E}$ of isotropically cracked bodies (Experimental results are plotted around the broken line derived from the self-consistent method which makes it possible to take into account the elastic interaction between cracks)

and 7, together with the theoretical lines of Eq. (27). Young's modulus $\bar{E}$ for isotropic samples are also shown in Fig. 8 in which the theoretical line of Eq. (28) is also given as a solid line. The following conclusions can be pointed out:

1) Roughly speaking, the cracked samples loses their elasticity with the increase of F_{11} or F_0 in accordance with Eqs. (27) and (28). Unfortunately, however, the theoretical lines are not exact to follow the experimental results, but rather give the upper bounds for the measured values (Fig. 6 and 8). This observation seems quite reasonable because the elastic interaction between cracks is neglected in the formulation of the equations.

2) The results of ν'/ν and $\bar{\nu}/\nu$ do not show any consistent trend, but are randomly distributed from 0.5 to 1.66. The measured values are apparently independent of the fabric tensor. The result might be partially because the measurement of $\bar{\varepsilon}_{22}$ is not accurate enough as compared with that of $\bar{\varepsilon}_{11}$. (The axial stress is transmitted through a rigid upper pedestal moving downward uniformly. The lateral expansion, on the other hand, freely occurs without any restriction which causes non-uniform lateral strain $\bar{\varepsilon}_{22}$.)

Self-Consistent Method for Cracked Bodies Having Isotropic Fabric

If attention is confined to isotropically cracked bodies ($F_{ij}=1/2F_0\delta_{ij}$), the self-consistent method is conveniently used to estimate the effect of the elastic interaction among cracks on the overall elastic compliance (Budiansky and O'Connell, 1976; Horii and Nemat-Nasser, 1983; Mura, 1982).

In the formulation of Eq. (24), the effect of cracks on the overall elastic behavior is considered by assuming that each crack is isolated from others in an isotropic elastic matrix of E and ν. The same formulation is adopted in the self-consistent method except that the elastic constants E and ν are simply replaced by the overall ones $\bar{E}$ and $\bar{\nu}$ respectively including the effect of cracks. This method is based on the thinking that the effect of the elastic interaction is already included in $\bar{E}$ and $\bar{\nu}$.

Using $\bar{E}$ and $\bar{\nu}$ in Eq. (23) $\bar{C}_{ijkl}$ becomes

$$\bar{C}_{ijkl}=\frac{\pi F_0}{8\bar{E}}(\delta_{il}\delta_{jk}+\delta_{ik}\delta_{jl}) \qquad (29)$$

since F_{ij} is set as $1/2F_0\delta_{ij}$ and cracks are considered elliptical. Using Eq. (29) in Eqs. (6) and (7), we have

$$\left[\left(\frac{1+\bar{\nu}}{\bar{E}}-\frac{1+\nu}{E}\right)\delta_{ik}\delta_{jl}-\left(\frac{\bar{\nu}}{\bar{E}}-\frac{\nu}{E}\right)\delta_{ij}\delta_{kl}\right]\bar{\sigma}_{kl}$$
$$=\frac{\pi F_o}{8\bar{E}}(\delta_{il}\delta_{jk}+\delta_{ik}\delta_{jl})\bar{\sigma}_{kl} \qquad (30)$$

Eq. (30) corresponds to

$$\frac{\bar{E}}{E}=\left(1-\frac{\pi}{4}F_o\right) \qquad (31\text{a})$$

and

$$\frac{\bar{\nu}}{\nu}=\frac{\bar{E}}{E} \qquad (31\text{b})$$

Eq. (31 a) is shown by broken line in Fig. 8.

Note that there is a marked tendency for the experimental points to be plotted around the broken line in the figure. When the elastic interaction becomes serious at high F_0, however, the experimental points seem to be plotted between the upper solid line and the lower broken line. Eq. (30) also suggests that the isotropically cracked body loses its elasticity if

$$F_o=\frac{4}{\pi}\cong 1.27 \qquad (32)$$

Look at Fig. 9 illustrating a crack pattern of $F_0=1.27$. Open cracks are set so closely that the cracked body probably loses its elasticity and should be treated as a granular material.

Results of Supersonic Wave Velocity Tests

Cylinder of gypsum plaster having 200 mm in diameter and 50 mm in height is casted, and is trimmed to make an equilateral polygon (Fig. 4 b). A generator and a receiver of supersonic wave are tightly pressed to the sample at diagonal positions. Supersonic wave velocity is determined in eight directions for each sample. Since shear wave is not measureable because of high damping of wave energy, longitudinal

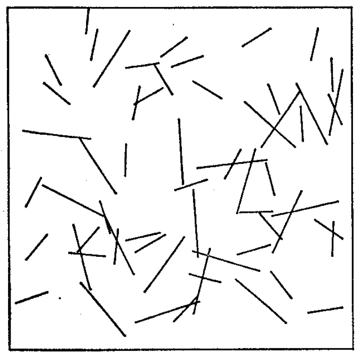

Fig. 9. A crack system having a zero-rank fabric tensor of 1.27

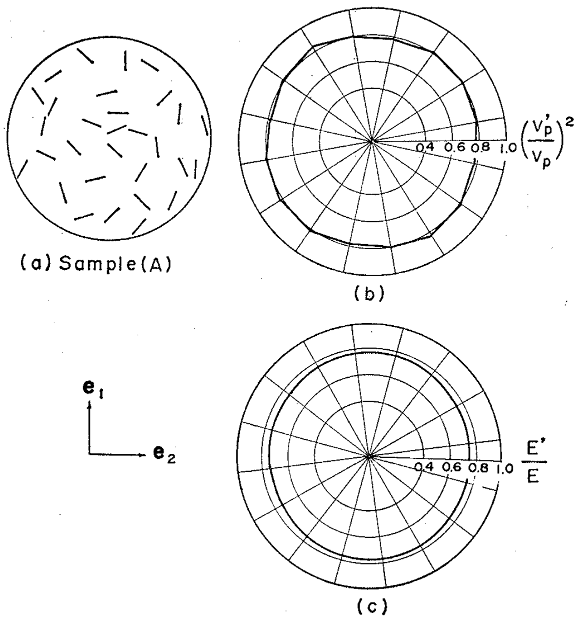

Fig. 10. Result of supersonic wave velocity test on sample (A) whose second-rank fabric tensor is considered isotropic

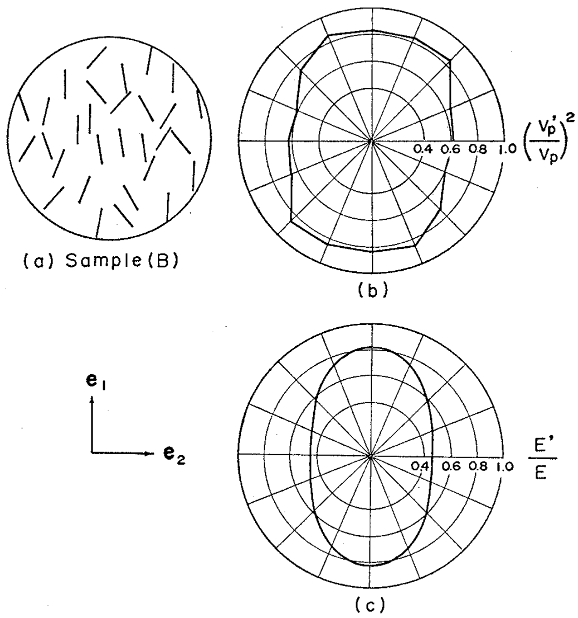

Fig. 11. Result of supersonnic wave velocity test on sample (B) whose crack geometry is intermediate between samples (A) and (C)

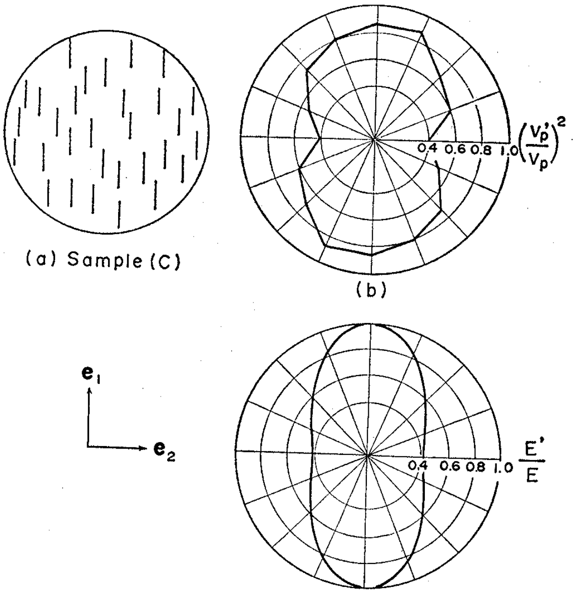

Fig. 12. Result of supersonic wave velocity test on sample (C) whose second-rank fabric tensor is strongly anisotropic due to completely parallel alignment of cracks

wave velocity v_v' is only reported here.

Three samples (A), (B) and (C) are chosen since they have different crack patterns (Figs. 10(a), 11(a) and 12(a)). Their fabric tensors $F_{ij}^{(A)}$, $F_{ij}^{(B)}$ and $F_{ij}^{(C)}$ are written below by setting the reference axes $\boldsymbol{e}_1$ and $\boldsymbol{e}_2$ parallel to the minor and major principal axes of the each fabric tensor respectively:

$$F_{ij}^{(A)}=\begin{bmatrix}0.182 & 0\\ 0 & 0.210\end{bmatrix}$$

$$F_{ij}^{(B)}=\begin{bmatrix}0.143 & 0\\ 0 & 0.739\end{bmatrix}$$

$$F_{ij}^{(C)}=\begin{bmatrix}0 & 0\\ 0 & 0.882\end{bmatrix}$$

Sample (A) is nearly isotropic, while sample (C) is distinctly anisotropic due to the parallel alignment of cracks. Sample (B) is intermediate between samples (A) and (B).

For an elastically isotropic body characterized by elastic constants E and ν, the longitudinal wave velocity v_p' is written as

$$(v_p')^2=\frac{E}{d}\frac{(1-\nu)}{(1+\nu)(1-2\nu)} \qquad (33)$$

where d is unit weight. A cracked body concerned here is elastically anisotropic because of the preferred alignment of cracks. Accordingly, Eq. (33) is not directly applicable to describe its wave velocity. It is reasonable to assume, as a rough approximation, that the square of wave velocity $(v_p')^2$ is proportional to the apparent Young's modulus E' for the corresponding direction:

$$(v_p')^2 \propto E' \qquad (34)$$

In Figs. 10(b), 11(b) and 12(b), the square $(v_v')^2$ of the measured longitudinal wave velocity, instead of v_v' itself, is given by normalizing it by the square of the longitudinal wave velocity of crack-free sample $(v_v)^2$.

For sample (A) having the slight anisotropic fabric tensor, $(v_v'/v_v)^2$ is almost independent of the measured direction. Accordingly, it behaves as an elastically isotropic material as being expected from the nearly isotropic fabric tensor $F_{ij}^{(A)}$. For samples (B) and (C) having the distinct anisotropic fabric tensor, on the other hand, $(v_v'/v_v)^2$ changes markedly from the maximum to the minimum velocities. It is of great importance to know that the maximum and the minimum wave velocities correspond to the minor and the major principal axes of the fabric tensor F_{ij} respectively. This result means the coaxiality between the principal axes of F_{ij} and the symmetry axes of $\bar{D}_{ijkl}$ as suggested by Eq. (24).

The conclusion that the wave velocity profiles are in good accordance with the crack geometry expressed by F_{ij} suggests one more important point. That is, geophysical prospecting can be used to estimate fabric tensors of in situ rock masses.

Theoretical Consideration

In Eq. (15), the local base vectors $\boldsymbol{e}_i'$ $(i=1,2)$ were related to the fixed base vectors $\boldsymbol{e}_i$ $(i=1,2)$ through an orthogonal tensor $\boldsymbol{Q}$. For a two-dimensional case, $\boldsymbol{Q}$ has components of

$$Q_{ij}=\begin{bmatrix}\cos\theta & \sin\theta\\ -\sin\theta & \cos\theta\end{bmatrix} \qquad (35)$$

where θ is an angle between $\boldsymbol{e}_1'$ and $\boldsymbol{e}_1$

(counterclockwise being positive). The elastic compliance $\bar{D}_{ijkl}$ must satisfy the following coordinate transformation rule:

$$\bar{D}_{mnop}'=Q_{mi}Q_{nj}Q_{ok}Q_{pl}\bar{D}_{ijkl} \quad (36)$$

where $\bar{D}_{mnop}'$ is defined with respect to the axes $\boldsymbol{e}_i'$ $(i=1,2)$. Using $\bar{D}_{ijkl}$ of Eq. (24) in Eq. (36), we have

$$\bar{D}_{mnop}'=\frac{1}{4D}(Q_{mi}Q_{pl}\delta_{no}F_{il}+Q_{mi}Q_{ok}\delta_{np}F_{ik}+Q_{nj}Q_{pl}\delta_{mo}F_{jl}+Q_{nj}Q_{ok}\delta_{mp}F_{jk})+\left[\frac{(1+\nu)}{E}\delta_{mo}\delta_{np}-\frac{\nu}{E}\delta_{mn}\delta_{op}\right] \quad (37)$$

Let us consider, for example, D_{1111}'. Eq. (37) becomes

$$\bar{D}_{1111}'=\frac{1}{D}Q_{1i}Q_{1j}F_{ij}+\frac{1}{E} \quad (38)$$

If a sample composed of elliptical cracks is compressed parallel to the direction of $\boldsymbol{e}_1'$, Eq. (38) becomes

$$\frac{E'}{E}=\frac{1}{\frac{\pi}{2}Q_{1i}Q_{1j}F_{ij}+1}=\frac{1}{\frac{\pi}{2}(F_{11}\cos^2\theta+2F_{12}\cos\theta\sin\theta+F_{22}\sin^2\theta)+1} \quad (39)$$

where

$$\frac{1}{D}=\frac{\pi}{2E}$$

and

$$E'=\frac{\bar{\sigma}_{11}'}{\bar{\varepsilon}_{11}'}$$

$\bar{\sigma}'_{11}$ and $\bar{\varepsilon}'_{11}$ are stress and strain components with respect to the local axes $\boldsymbol{e}_i'$ $(i=1,2)$.

Figs. 10(c), 11(c) and 12(c) show the change of E'/E by the angle for the three samples (A), (B) and (C). Note that the profiles of E'/E are quite similar to those of $(v_p'/v_p)^2$. Accordingly, Eq. (24) is proved to be applicable, at least in a qualitative manner, to show the elastic compliance of real cracked materials.

CONCLUSIONS

Elastic compliance for cracked materials like rocks and rock masses is theoretically formulated in terms of the generalized fabric tensor which has been introduced as an index measure to express explicitly the crack geometry. By means of uniaxial compression tests and supersonic wave velocity tests on gypsum plaster samples with random cracks, the formulation is proved to be a good approximation for describing the elastic response of cracked materials. The conclusions are summarized as follows:

1) The principal axes of the fabric tensor of second-rank exactly coincide with the symmetry axes of the elastic compliance tensor of fourth-rank.

2) The so-called self-consistent method is very useful to estimate the overall elastic moduli by taking into account the effect of elastic interaction among cracks.

3) Since the supersonic wave velocity is closely related to the character of the fabric tensor, it can be expected that the field measurement of wave velocity is useful to estimate fabric tensor of in situ rock masses.

ACKNOWLEDGMENT

The authors express their sincere gratitude to Mr. R. Nozaki of Central Research Institute of Electric Power Industry for giving us an opportunity to measure supersonic wave velocity of cracked materials.

NOTATION

$\bar{C}_{ijkl}$=elastic compliance tensor due to presence of cracks

$\bar{D}_{ijkl}$=elastic compliance tensor for a cracked body

$\boldsymbol{e}_i(i=1,2,3)$=fixed base vectors

$\boldsymbol{e}'_i(i=1,2,3)$=local base vectors

E=Young's modulus for isotropic matrix without a crack

$\bar{E}$=Young's modulus for an isotropically cracked body

E'=apparent Young's modulus for an

anisotropically cracked body

$E(\boldsymbol{n}, r)$ = probability density function to describe orientation of cracks

$f(r)$ = probability density function to describe size of cracks

$\boldsymbol{F}$ = generalized fabric tensor

F_0 = fabric tensor of zero-rank

F_{ij} = fabric tensor of second-rank

F_{ijkl} = fabric tensor of fourth-rank

$m^{(V)}$ = number of cracks in volume V

$\boldsymbol{m}$ = unit vector normal to a crack surface

$\bar{M}_{ijkl}$ = elastic compliance tensor for elastic matrix

$\boldsymbol{n}$ = unit vector normal to the major principal plane of a crack

$\boldsymbol{Q}$ = orthogonal tensor to relate $\boldsymbol{e}_i'$ to $\boldsymbol{e}_i$

$2S(r)$ = total surface area of cracks

$\boldsymbol{u}$ = displacement vector

V = volume

v_p = longitudinal wave velocity

α_{ij} = crack density tensor by Kachanov

$\boldsymbol{\delta}$ = displacement jump vector

δ_{ij} = Kronecker's delta

$\bar{\varepsilon}_{ij}$ = average strain tensor

θ = angle between $\boldsymbol{e}_1$ and $\boldsymbol{e}_1'$

ν = Poisson's ratio for isotropic matrix without a crack

$\bar{\nu}$ = Poisson's ratio for an isotropically cracked body

ν' = apparent Poisson's ratio for an anisotropically cracked body

ρ = volume density of cracks

$\bar{\sigma}_{ij}$ = average stress tensor

Ω = solid angle equivalent to an entire unit sphere

REFERENCES

1) Brown, E. T. (1970) : "Strength of models of rock with intermittent joints," J. Soil Mech. Fdn. Div. Am. Inst. Civ. Engrs., Vol. 96, SM 6, pp. 1935-1946.

2) Budiansky, B. and O'Connell, R. J. (1976) : "Elastic moduli of a cracked solid," Int. J. Solids Struct., Vol. 12, pp. 81-97.

3) Cundall, P. A. (1971) : "A computer model for simulating progressive, large-scale movements in blocky rock system," Proc. Symp. Int. Soc. Rock Mech., Nancy 2, art 8.

4) Eimer, CZ. (1978) : "Elasticity of cracked medium," Archives Mechanics, Archiwum Mechaniki Stosowanej, Vol. 30, No. 6, pp. 827-836.

5) Einstein, H. H. and Hirschfeld, R. C. (1973) : "Model studies on mechanics of jointed rock," J. Soil Mech. Fdn. Div. Am. Inst. Civ. Engrs., Vol. 99, SM 3, pp. 229-248.

6) Goodman, R. E., Taylor, R. L. and Brekke, T. L. (1968) : "Model for the mechanics of jointed rock," J. Soil Mech. Fdn. Div. Am. Inst. Civ. Engrs., Vol. 94, SM 3, pp. 637-659.

7) Hansagi, J. (1974) : "A method of determining the degree of fissuration of rock," Int. J. Rock Mech. Min. Sci. & Geomech. Abstr., Vol. 11, pp. 379-388.

8) Hayashi, M. (1966) : "Strength and dilatancy of brittle jointed mass : The extreme value stochastics and anisotropic failure mechanism," Proc. Ist Cong. Int. Soc. Rock Mech., Lisbon 1, pp. 295-302.

9) Horii, H. and Nemat-Nasser, S. (1983) : "Overall moduli of solids with microcracks : load induced anisotropy," J. Mech. Phys. Solids, Vol. 31, No. 2, pp. 155-171.

10) Horii, H. (1983) : "Overall response and failure of brittle solids containing micro-cracks,"Ph. D thesis, Northwestern University.

11) Hudson, J. A. and Priest, S. D. (1983) : "Discontinuity frequency in rock masses," Int. J. Rock Mech. Min. Sci. & Geomech. Abstr., Vol. 20, No. 2, pp. 73-89.

12) Jaeger, J. C. and Cook, N. G. W. (1968) : Fundamental Rock Mechanics, Methuen & Co. Ltd.

13) John, K. W. (1962) : "An approach to rock mechanics," J. Soil Mech. Fdn. Div. Am. Inst. Civ. Engrs., Vol. 88, SM 4, pp. 1-30.

14) Kachanov, M. (1980) : "Continuum model of medium with cracks," J. Engrg. Mech. Div. Am. Inst. Civ. Engrs., Vol. 106, SM 5, 1039-1051.

15) Kachanov, M. (1982) : "A micro-crack model of rock in elasticity (Part I : Frictional sliding on micro-cracks)," Mechanics of Materials, Vol. 1, pp. 19-27.

16) Kawai, T. and Takeuchi, N. (1983) : "New discrete models and their application to mechanics of granular materials," Studies in Applied Mechanics 7, Mechanics of Granular Materials (Edited by Jenkins and Satake), Elsevier, pp. 151-172.

17) Kiraly, L. (1969) : "Statistical analysis of fracture (orientation and density)," Geol. Rundsch, Vol. 59, No. 1, pp. 125-151.

18) Mura, T. (1982) : "Micromechanics of Defects in Solids," Martinus Nijhoff Publ., The Hague, Boston.

19) Oda, M., Nemat-Nasser, S. and Mehrabadi, M. M. (1982) : "A statistical study of fabric in a random assembly of spherical granules," Int. J. Numer. Anal. Methods Geomech., Vol. 6, pp. 77-94.

20) Oda, M. (1982) : "Fabric tensor for discontinuous geological materials," Soils and Foundations, Vol. 22, No. 4, pp. 96-108.

21) Oda, M. (1983) : "A method for evaluating the effect of crack geometry on the mechanical behavior of cracked rock masses," Mechanics of Materials, Vol. 2, No. 2, pp. 163-171.

22) Oda, M. (1984): "Similarity rule of crack geometry in statistically homogeneous rock masses," Mechanics of Materials, Vol. 3.

23) Ogata, S. (1978) : "Quantitative characterization of distribution parameters of joints in rock masses," Engineering Geology, J. Japan Soc. Engrg. Geol., Vol. 19, No. 1, pp. 12-20 (in Japanese).

24) Onodera, T., Yoshinaka, R. and Oda, M. (1974) : "Weathering and its relation to mechanical properties of granite," Proc. 3rd Int. Congr. Rock Mech., Vol. 2, pp. 71-78.

25) Patton, F. D. (1966) : "Multiple modes of shear failure in rock," Proc. 1st Congr. Int. Soc. Rock Mech., Lisbon, Vol. 1, pp. 509-513.

26) Silveria, A. F., Rodrigues, F. P. and Grossmann, N. F. (1966) : "Quantitative characterization of the geometric parameters of jointing in rock masses," Proc. 1st Congr. Int. Soc. Rock Mech., Lisbon, Vol. 1, pp. 225-233.

27) Sneddon, I. N. and Lowengrub, M. (1969) : Crack Problems in the Classical Theory of Elasticity, The SIAM Series in Applied Mechanics, John Wiley & Sons, Inc.

28) Sprunt, EVE S. and Brace, W. F. (1974): "Direct observation of microcavities in crystalline rocks," Int. J. Rock Mech. Min. Sci. & Geomech. Abstr., Vol. 11, pp. 139-150.

29) Walsh, J. B. (1965 a) : "The effect of cracks on the compressibility of rock," J. Geophy. Research, Vol. 70, No. 2, pp. 381-389.

30) Walsh, J. B. (1965 b): "The effect of cracks on the uniaxial elastic compression of rocks," J. Geophy. Research, Vol. 70, No. 2, pp. 399-411.

31) Yoshinaka, R., Yamabe, T. and Sekine, I. (1982) : "Experimental and numerical studies on discontinuous rock mass : evaluation of equivalent deformation moduli," Report of Dept. Found Engrg. & Const. Engrg., Saitama University, Vol. 12, pp. 67-85.

32) Zienkiewicz, O. C. and Dullage, C. (1970) : "Analysis of non-linear problems in rock mechanics with particular reference to jointed rock systems," Proc. 2nd Int. Congr. Rock Mech., Vol. 3, pp. 501-509.